

## Microfluidic lab-on-a-chip systems based on polymers— fabrication and application

Andreas E. Guber<sup>a,\*</sup>, Mathias Hecke<sup>a</sup>, Dirk Herrmann<sup>a</sup>, Alban Muslija<sup>a</sup>, Volker Saile<sup>a</sup>,  
Lutz Eichhorn<sup>b</sup>, Thomas Gietzelt<sup>b</sup>, Werner Hoffmann<sup>c</sup>, Peter C. Hauser<sup>d</sup>,  
Jatisai Tanyanyiwa<sup>d</sup>, Andreas Gerlach<sup>e</sup>, Norbert Gottschlich<sup>e</sup>, Günther Knebel<sup>e</sup>

<sup>a</sup> Forschungszentrum Karlsruhe GmbH, Institut für Mikrostrukturtechnik, 76021 Karlsruhe, Germany

<sup>b</sup> Forschungszentrum Karlsruhe GmbH, Institut für Mikroverfahrenstechnik, 76021 Karlsruhe, Germany

<sup>c</sup> Forschungszentrum Karlsruhe GmbH, Institut für Instrumentelle Analytik, 76021 Karlsruhe, Germany

<sup>d</sup> Department of Chemistry, University of Basel, 4004 Basel, Switzerland

<sup>e</sup> Greiner Bio-One GmbH, 72636 Frickenhausen, Germany

### Abstract

In the future, plastic-based lab-on-a-chip systems will play a crucial role in modern life sciences, e.g. biotechnology and (bio)medical engineering. Presently, microfluidic systems for capillary electrophoresis (CE) are being used. They allow for the safe handling of smallest substance volumes in the pL range and their separation into the individual components. From the microtechnical point of view, current R&D activities mainly focus on the development of inexpensive fabrication methods. Low-cost CE systems may be obtained by plastic molding techniques on a polymer basis. First separations of biological fluids and inorganic ion solutions have been performed successfully. © 2004 Elsevier B.V. All rights reserved.

**Keywords:** Microfluidic systems; Lab-on-a-chip; Capillary electrophoresis; CCD Technique

### 1. Introduction

Microfluidic systems increasingly gain importance in modern life sciences as well as in diagnostic and therapeutic biomedical engineering.

Special types of microfluidic and nanofluidic structures are applied in so-called micro total analysis systems ( $\mu$ TAS) [1] and lab-on-a-chip systems [2], in miniaturized drug delivery systems as well as in areas of tissue engineering [3].

These are predominantly passive microcomponents, e.g. simple microdepressions that are frequently applied in conventional microtiter plates as reservoir areas or miniaturized sample chambers, so-called wells. Miniaturized analysis systems are additionally equipped with capillary microchannel structures, mainly in the form of inlet or supply channels or as reaction or separation sections. Microchannels with integrated microcomponents may take over either mixing or filter functions. Via smallest pores, a precisely adjusted sample transfer into and from microfluidic systems can be achieved [4].

Active microcomponents comprise, e.g. smallest pumping or valve systems that are mostly found in rather complex  $\mu$ TAS systems [5].

Hence, lab-on-a-chip systems represent special  $\mu$ TAS systems that are usually designed for a certain and well-defined analytical task. As presently there is a considerable need for miniaturized separation systems in various areas of modern life sciences (biotechnology, pharmaceutical industry, etc.), miniaturization of capillary electrophoresis (CE) also is in the focus of interest. CE systems currently represent a major example of use of microfluidic systems. By means of CE technology, substance mixtures of various biomolecules (DNA, proteins, etc.) or inorganic ions can be separated specifically into their components.

To meet the requirements of modern substance research, future lab-on-a-chip systems for CE technology also will have to be suitable for use in high-throughput screening (HTS) and ultra-high-throughput screening (UHTS). It is therefore required to implement microfluidic structures on the standardized format of microtiter plates, with the fabrication on the basis of microtechnically processed polymer substrates being rather inexpensive. For reasons of costs and hygiene, single-use products made of biocompatible polymers offer considerable advantages.

\* Corresponding author.

E-mail address: andreas.guber@imt.fzk.de (A.E. Guber).

## 2. Setup and function of lab-on-a-chip systems for capillary electrophoresis

The setup and functioning principle of a microfluidic system for capillary electrophoresis is represented schematically in Fig. 1. The most simple design of such a system consists of two intersecting microchannels that can be reached via reservoir areas (Fig. 1a). After buffer solution has been introduced into the entire microfluidic CE system, the shorter channel serves as a sample channel for the sample material to enter the area of capillary intersection. This is achieved by means of an electric field applied between the sample reservoir and the sample waste reservoir. The sample mixture to be separated is transported through the entire sample channel (Fig. 1b). For this purpose, either the respective electrodes have to be lowered into the reservoir areas from above or electric conduction paths have to be integrated directly on the CE chip. Following electric switching, the sample volume located in the intersection area is injected into the separation channel. There, the plug is separated into its components depending on the electric charge and the molecule size (Fig. 1c). Optical or electrochemical detection usually takes place at the end of the separation channel (Fig. 1a).

All lab-on-a-chip systems presented here are microfluidic CE systems. For reasons of handling, it is recommended to arrange these miniaturized CE systems on generally and easily accessible, standardized platforms. At the moment, two major approaches are pursued. CE systems may be arranged on smaller base formats (e.g. on the microscope slide format; 25 mm × 75 mm) or on the area of standard microtiter

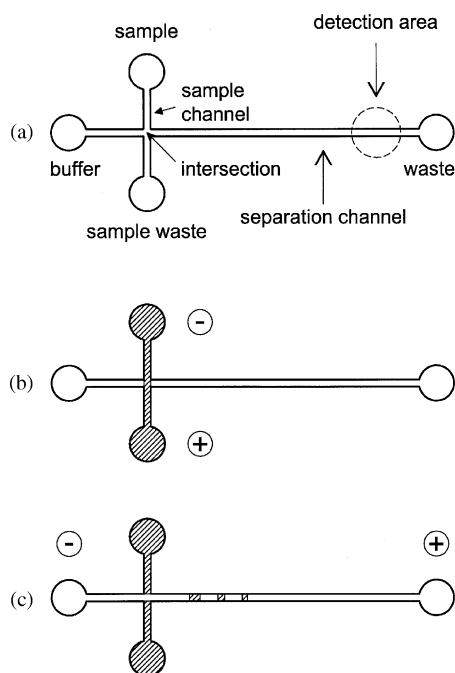


Fig. 1. Setup and functioning principle of a lab-on-a-chip systems for capillary electrophoresis.

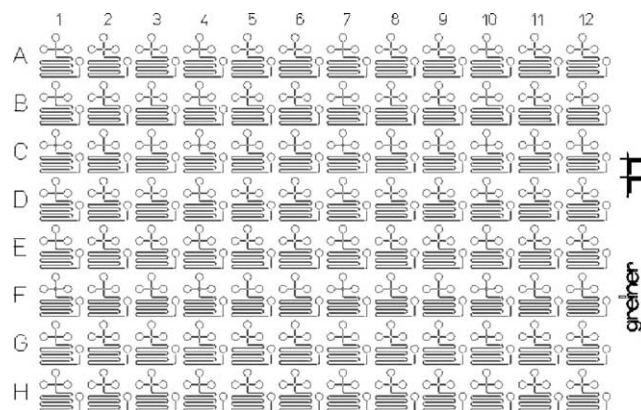


Fig. 2. Schematic representation of a microtiter plate with 96 identical CE systems.

plates (125 mm × 85 mm). Principle arrangement of 96 identically designed CE systems on the format of a microtiter plate is shown schematically in Fig. 2. For reasons of space, all CE systems are equipped with a meandering separation channel in this case [6].

Electric contacting of all 96 CE systems is achieved by conduction paths integrated on the microtiter plate and extending into the respective reservoir areas (Fig. 9). These novel microtiter plates for the first time allow for up to 96 simultaneous CE separations being accomplished in a single process step according to the HTS concept.

## 3. Microtechnical fabrication and assembly

To produce microfluidic modules and systems from polymers, various microtechnical fabrication methods have been made available in the meantime [7]. For the low-cost production of plastic microcomponents, replication methods, e.g. hot embossing, injection molding or injection embossing, are applied [7,8]. However, this results in the necessity of producing a metal mold insert possessing the inverse microfluidic structures. Depending on the requirements to be fulfilled by the design of the microfluidic structural details and the total base area to be processed, various fabrication methods can be employed for the construction of metal molds. If necessary, these fabrication methods can also be used in a complementary manner. The LIGA process or UV lithography coupled with electrodeposition allow for the manufacture of nickel mold inserts with extremely filigree structural details (minimum dimensions <math><1\ \mu\text{m}</math>). Large-area mold inserts of brass or steel can be produced by means of microcutting [9] or the  $\mu\text{EDM}$  technique [10]. Here, the size and shape of the microtools (monocrystalline microdiamonds or thin cutting wires) determine the structural details to be generated on the mold inserts (minimum dimensions between 20 and 50  $\mu\text{m}$ , depending on the fabrication method).

Fig. 3 presents a general view of a mold insert that was cut into a round semi-finished brass block using the microcutting



Fig. 3. General view of the metal mold insert made of brass with three identical fabrication areas.

method. According to the space available, up to three inverse microfluidic structures (in the microscope slide format each) can be arranged side by side as raised microstructures on the mold insert. Thus, component yield during hot embossing is increased and cycle times per CE structure molded are shortened indirectly.

The SEM in Fig. 4 shows the inverse microstructure of an offset double-T junction, by means of which the injection volume of the molded CE chip is increased. The cross-

section amounts to  $50\ \mu\text{m} \times 50\ \mu\text{m}$ . For reasons of fabrication, the radius of the “round corners” is  $25\ \mu\text{m}$  at the minimum. Hence, an injection volume of about 650 nl results according to pure calculation. Exact geometrical design of the capillary intersection area is of importance for the exact operation of CE systems, as it determines the respective injection volume. The milling traces left on the structure ground by the  $50\ \mu\text{m}$  hard-metal mill are clearly visible in Fig. 4. Roughness of the side walls amounts to about 200 nm.

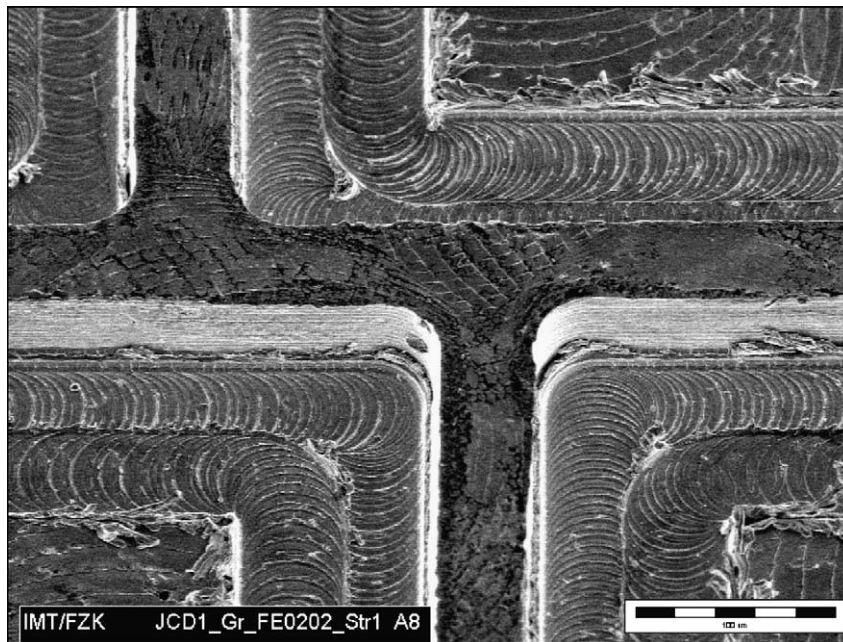


Fig. 4. SEM of the offset double-T junction in the area of the capillary cross.



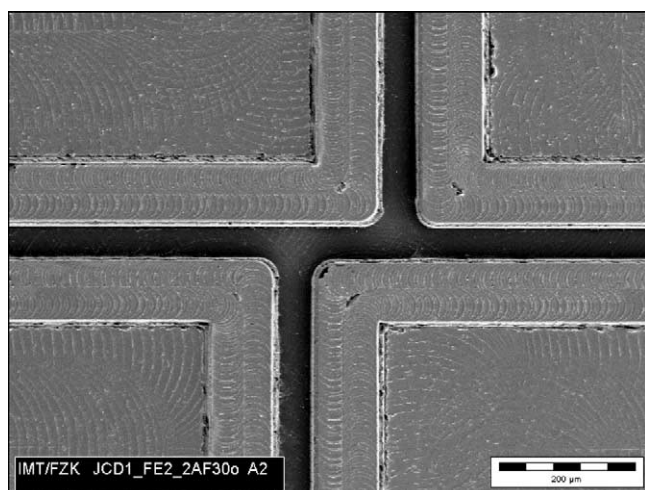


Fig. 5. SEM of a PMMA microchannel system with an integrated double-T channel junction molded by hot embossing.

Brass tools with various channel designs can be molded into PMMA, COC, and PS by means of the replication techniques available (vacuum hot embossing or micro injection molding). The double-T junction area molded into PMMA is shown in Fig. 5. It was found out by detailed evaluations using a special high-performance light microscope that the required channel widths and depths ( $50\ \mu\text{m}$  each) are observed exactly in the entire CE system.

For mass fabrication the performance of the prototyping technique hot embossing is not sufficient compared to fully automated injection molding. Cycle times can be reduced by a factor of about ten using injection molding. Fig. 6 presents a detailed view of the of a COC meandering microchannel of the CE system shown in Fig. 2. Using the design presented here, channel width is reduced from 100 to about  $50\ \mu\text{m}$ . After passing a “ $180^\circ$  turn”, the channel cross-section widens again. As a result of this constructive measure, formation of undefined flow fronts of already separated biomolecules

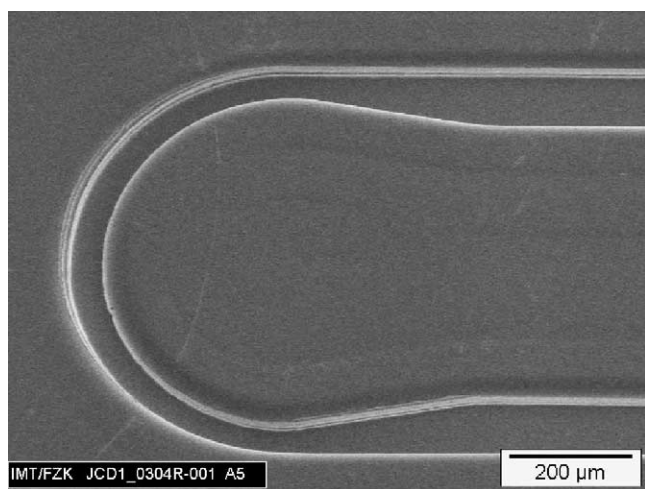


Fig. 6. SEM of a COC microchannel system molded using the micro injection molding technique.

can be reduced significantly during electrophoretic separation [11].

To obtain real capillary systems, however, the replication process has to be followed by a cover process, during which all fluidic microchannel systems are closed in a precise and leakage-free manner. For this purpose, exactly adapted cover plates with previously cut-in penetration holes are used. During later use of the CE systems, all reservoir areas of the microchannels will have to be reached via these holes. In the case of microtiter plates with 96 CE systems, for instance, the cover plate has to be provided with a total of 384 penetration holes. Depending on the polymer materials used, two bonding techniques (solvent bonding or UV bonding) are available for this purpose.

In solvent bonding [12] the surfaces of both polymer parts are slightly wetted and, thus, loosened using specially tailored solvent mixtures. In a special device, both components are then positioned opposite to each other with the help of adjustment pins or bores and joined permanently under pressure. As a drawback of this technology, all surfaces—also the later microcapillary structures—are entirely exposed to the solvents used. This may result in a modification of the microchannel surface properties.

In the case of UV-supported bonding [13,14], surfaces of the microstructured substrate and cover plate are first exposed to a dosed UV radiation which considerably reduces the glass transition temperature of the polymer materials in the microcomponent areas that are located close to the surface. Subsequently, the base plate and cover plate are joined tightly under force and heat. A covered CE chip tailored to the outer dimensions of a microscope slide is shown in Fig. 7. Fig. 8 presents the SEM of a  $100\ \mu\text{m}$  wide and  $50\ \mu\text{m}$  high microchannel covered by the technique described above. Tightness of all microcapillary structures can be checked easily by simple filling tests with colored aqueous media [6].

For the electric control of the CE systems, tiny electrodes can be lowered into the reservoir areas. In case of a microtiter plate with 96 CE systems, a total of 384 electric conductor paths are located on the two levels of the chip setup plate to prevent electrode cross contacts (Fig. 9). Possibly required electric thin-film electrodes of gold are generated by sputtering and using adapted shadow masks. They are sputtered onto a chromium adhering layer and have a width of about  $200\ \mu\text{m}$  and a height of  $250\ \text{nm}$ .

The CE systems produced so far have either a meandering or a linear separation channel of 40–80 mm length. On the microscope slide format, one or two CE systems are



Fig. 7. Covered CE chip in the microscope slide format.

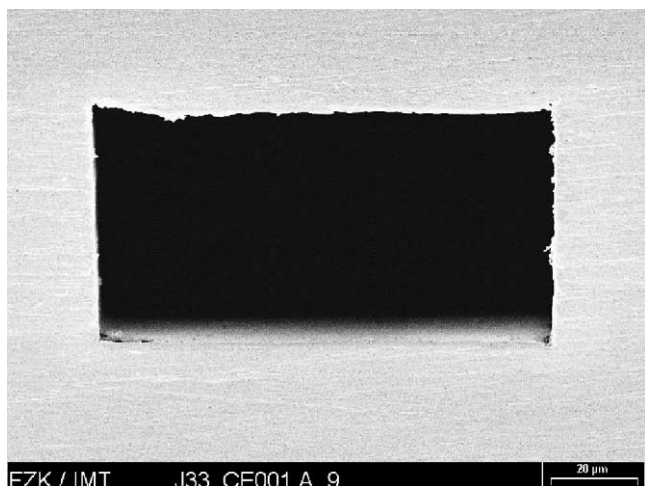


Fig. 8. SEM of the channel cross-section.

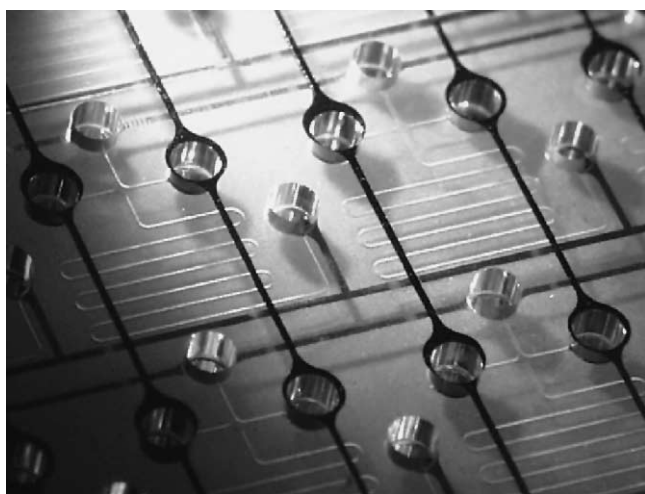


Fig. 9. Detailed representation of electric contacting of the CE structures via the reservoir areas on a microtiter plate. Each CE unit can be controlled via four individual gold conduction paths.

arranged with partly offset crossing areas (T-junctions). In the case of microtiter plates, a total of 96 identically designed CE systems are available on one plate. Generally, the channel cross-section may be set in wide ranges. For the systems presented here, it varies between  $50\ \mu\text{m} \times 50\ \mu\text{m}$  and  $100\ \mu\text{m} \times 50\ \mu\text{m}$ .

#### 4. CE separations in lab-on-a-chip systems

At the end of the separation capillaries, detection can be carried out with light-optical methods (e.g. fluorescence spectroscopy techniques) or with an electric measurement (Fig. 1a). For electric conductivity detection, the measurement electrodes are integrated in the microchannels. In the contactless conductivity detection (CCD technique) mode, they are arranged outside.

The CE systems available (cf. Figs. 7 and 9) may be subjected to simple separation tests of charged particles in an electric field. After filling the entire CE structure with an agarose gel, for example, a sample mixture of DNA and a dye can be introduced into the sample channel via the sample reservoir using an electric field of 500 V. After having filled the intersection area with the sample, the electric field is changed. Injection of the fluorescent dye into the separation channel starts after about 4 s. With increasing time, the generated plug is transported further into the separation channel (Fig. 10). When operating the CE chips, the electric fields applied must be prevented from generating undesired electrolysis effects that lead to a massive bubble formation in the channel systems. These bubbles may cut off further substance flow in the fine separation channels.

In other experiments on electrokinetic injection,  $1\ \mu\text{mol}$  fluorescent dye (sulforhodamine B) was injected at a voltage of 420 V/cm. Prior to this, the entire channel system had been filled with a separation matrix consisting of 3% linear polyacrylamide in TRIS–borate EDTA buffer. Detection took place at a distance of about 10 mm from the capillary cross. For excitation, an Nd:YAG laser was applied. About

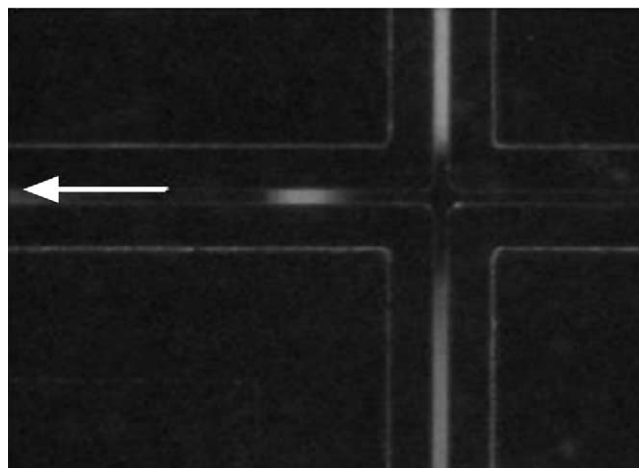
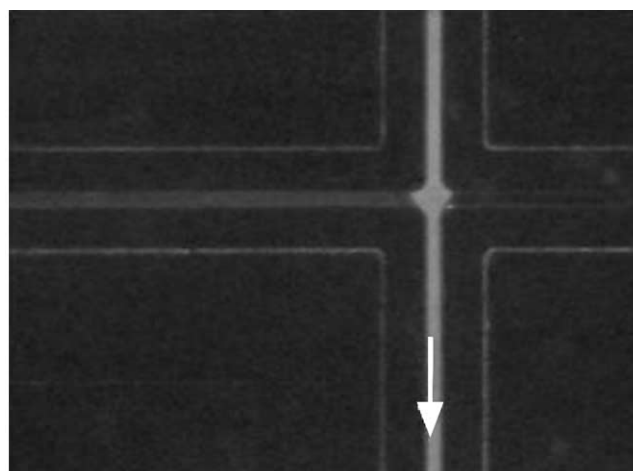


Fig. 10. Injection of a fluorescent dye into the separation channel.

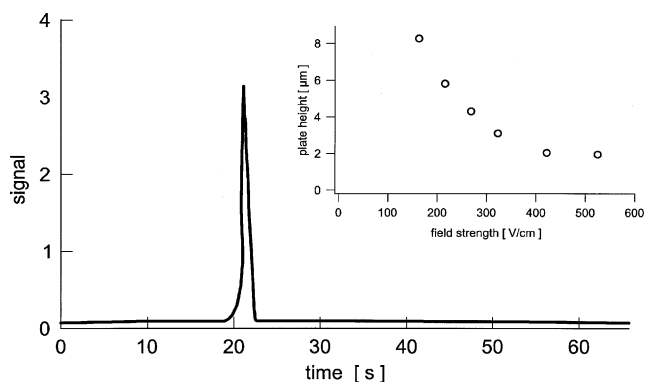


Fig. 11. Detection of Sulfurhodamine B in the separation channel. The inset shows the plate height as a function of the separation field strength.

20–25 s after injection, a clear signal of the fluorescent dye was detected (Fig. 11) [15]. In the meantime, also a mixture of DNA fragments in the range of 100–1000 bp has been separated successfully after a few millimeters by applying an electric field (160 V/cm) in the separation section. (Data not shown).

In addition, experiments on the conductivity detection of inorganic cations and anions have been performed in CE systems made of PMMA. In principle, conductivity can be measured by electrodes integrated in the separation channel and strongly miniaturized on a CE chip [16]. However, in previous experiments, it was demonstrated, that an integration of measurement electrodes at the end of a separation channel is not always optimal. Depending on the substance mixtures to be separated, the gold electrodes may be damaged massively—especially when continuously operating the CE system over a period of several hours up to several days—such that the entire CE chip cannot be used any longer.

This may be avoided by using a contact-free capacitive conductivity detection technique (CCD technique). Here, the measurement electrodes no longer are in direct contact with the fluid. The electrodes are arranged outside of the separation channel and located a little below the channel system only. Hence, the CE chip applied has to possess an extremely thin cover plate. In the studies presented here, it is only 40 μm thick. The measurement setup is represented schematically in Fig. 12. The measurement electrodes are located in a holding unit on a base plate. Then, the assembled CE chip with the thin cover plate is put onto the electrodes and fixed for measurement.

Fig. 13 shows an electropherogram obtained by means of the CCD technique. A mixture of four alkaline cations ( $\text{Rb}^+$ ,  $\text{K}^+$ ,  $\text{Na}^+$ ,  $\text{Li}^+$ ) with a concentration of 10 μM was separated successfully. 10 mM of MES-His buffer (MES: 2-(*N*-morpholino)ethanesulfonic acid; His: histidine) with 4 mM of 18-crown-6 at a pH of 6.0 was applied as buffer solution [17]. This type of separation of a cation mixture could be reproduced several times over a longer period (e.g. 4 weeks) with the same chip. No marked changes of detection sensi-

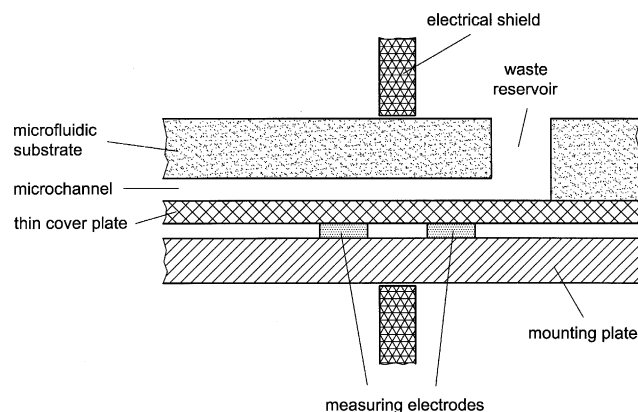


Fig. 12. Cross-section of the measurement setup used for contact-free conductivity detection. The two measurement electrodes are located outside of the separation channel at the end.

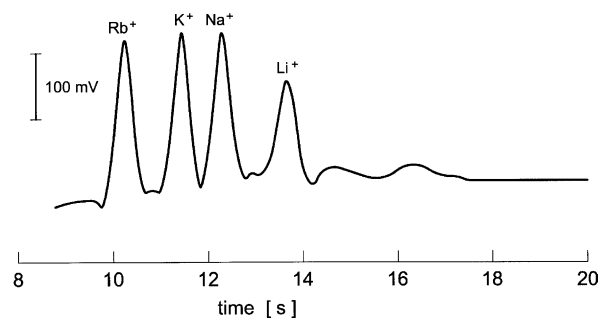


Fig. 13. Electropherogram of four separated alkaline cations.

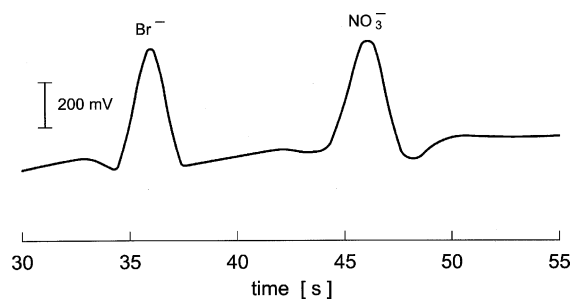


Fig. 14. Electropherogram of two separated inorganic anions.

tivity were noticed. The lower detection limit for the cations amounted to about 2 μM. In addition, a mixture of two anions was separated in the CE chip. Concentration of the anions amounted to 50 μM in 10 mM of MES-His buffer. The respective electropherogram is shown in Fig. 14.

## 5. Summary and outlook

Meanwhile, a large number of microfluidic CE systems have been produced at Forschungszentrum Karlsruhe within the framework of a first prototype series. Using the brass mold inserts available and an optimized vacuum hot embossing technique or injection molding techniques, exact



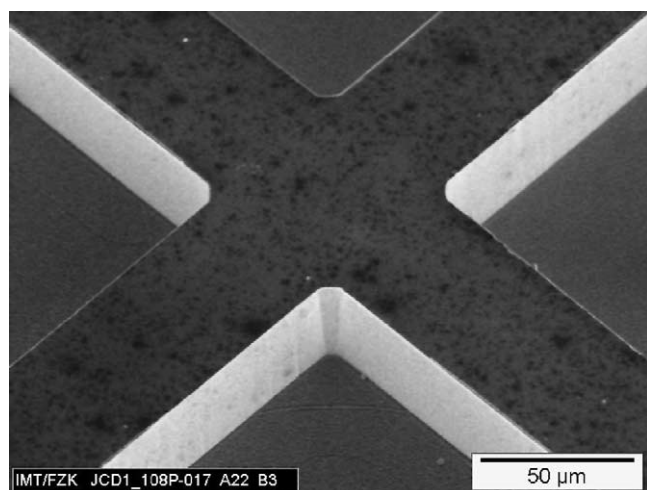


Fig. 15. Detailed view of an intersection of two inverse microstructures made of nickel, which are 50 μm in height and width.

replication of all fluidic CE channel systems in PMMA, PS, and COC was achieved. To obtain real capillary systems, all fluidic microchannel systems are closed in a precise and leakage-free manner. Depending on the polymer materials used, two bonding techniques are available for this purpose. Possibly required electric thin-film electrodes of gold are generated by sputtering and using adapted shadow masks. In the case of the microtiter plates, the thin-film electrodes to control capillary electrophoresis are arranged on two different levels of the chip setup for reasons of space and to prevent electrode cross contacts.

The fluidic tests performed revealed a good filling behavior for liquids and gels needed for separation. By applying electric fields, a test mixture of DNA and dye can be introduced into the sample channel and a small sample plug can be injected into the separation channel. Furthermore, electrophoretic separation of inorganic cations and anions and their detection by CCD could be demonstrated.

Hence, the PMMA, PS or COC CE systems presented here are suited in principle for practical use in many fields of bioanalysis and inorganic ion analysis. Future research and development work therefore will be aimed at implementing novel lab-on-a-chip systems that contain additional integrated sub-systems for, e.g. continuous preliminary cleaning of the sample and sample preparation. On the other hand to extend their potential use, novel fields of application, such as mobile analysis, will have to be opened up for the above chip systems. For instance, the use for multi-element analysis based on electrophoretic ion separation may be considered.

As far as fabrication and the exact design of the capillary intersection are concerned, it has been succeeded in generating a nickel-molding tool by means of the UV-LIGA technique. Using this tool, a channel intersection with nearly

perfectly shaped 90° corners can be obtained (Fig. 15) which should provide formation of well-defined sample plugs.

## Acknowledgements

The authors would like to thank Messrs. H. Biedermann and A. Mayer (both IMT), D. Scherhauser (IMVT) for their constant support in the rapid fabrication of the above lab-on-a-chip systems. Thanks go to Dr. H. Hein (IMT) for the fabrication of the mold inserts by UV lithography and nickel electroplating. Thanks are also due to Mr. P. Abaffy (IMT) for the large number of SEMs made as well as for the evaluation of a number of light-optical images to determine the exact channel cross-sections.

## References

- [1] A. van den Berg, W. Olthuis, P. Berveld (Eds.), *Proceedings of the μTAS Symposium 2000*, Kluwer Academic Publishers, Dordrecht, The Netherlands, 2000.
- [2] H. Becker, C. Gärtner, *Physikalische Blätter* 55 (6) (1999) 51.
- [3] S. Giselbrecht, E. Gottwald, G. Knedlitschek, K.F. Weibezahn, A. Welle, A.E. Guber, D. Herrmann, A. Muslija, W.K. Schomburg, *Biomedizinische Technik* 47 Ergänzungsband 1 (2002) 373.
- [4] A.E. Guber, H. Dittrich, M. Hecke, D. Herrmann, A. Muslija, W. Pflüger, Th. Schaller, in: J.M. Ramsey, A. van den Berg, (Eds.), *Proceedings of the μTAS Symposium (μTAS 2001)*, Kluwer Academic Publishers, Dordrecht, The Netherlands, 2001, p. 155.
- [5] F. Völklein, T. Zetterer, *Einführung in die Mikrosystemtechnik—Grundlagen und Praxisbeispiele*, Friedr. Vieweg & Sohn-Verlag Braunschweig, 2000.
- [6] A.E. Guber, M. Hecke, D. Herrmann, A. Muslija, Th. Schaller, A. Gerlach, G. Knebel, in: M. Matlosz, W. Ehrfeld, J.P. Baselt (Eds.), *Proceedings of the Fifth International Conference on Microreaction Technology (IMRET5)*, Springer-Verlag, Berlin, Heidelberg, Germany, 2002, p. 532.
- [7] W. Menz, J. Mohr, O. Paul, *Microsystem Technology*, Wiley-VCH-Verlag, Weinheim, 2001.
- [8] M. Hecke, W. Bacher, *NACHRICHTEN Forschungszentrum Karlsruhe* 30 (3–4) (1998) 231.
- [9] W. Pflüger, T. Schaller, *NACHRICHTEN Forschungszentrum Karlsruhe* 34 (2–3) (2002) 210.
- [10] A.E. Guber, D. Herrmann, A. Muslija, *Med. Devices Technol.* 4 (2001) 22.
- [11] E.T. Lagally, B.M. Paegel, R.A. Mathies, in: *Proceedings of the μTAS Symposium*, Kluwer Academic Publishers, Dordrecht, The Netherlands, 2000, p. 217.
- [12] P. Volk, R. Bader, P. Jacob, H. Moritz, *DE 19851644 A1* (1999).
- [13] Patent pending.
- [14] R. Truckenmüller, P. Henzi, D. Herrmann, V. Saile, W.K. Schomburg, in: *Proceedings of the Symposium on Design, Test, Integration and Packaging of MEMS/MOEMS*, 2003, 265.
- [15] N. Gottschlich, A. Gerlach, G. Knebel, D. Herrmann, A.E. Guber, M. Hecke, A. Muslija, L. Eichhorn, T. Schaller, *Conference Handbook IBC Microfluidics Conference*, 2002.
- [16] F.-M. Matysik, *Nachrichten aus der Chemie* 48 (2000) 632.
- [17] J. Tanyaniwa, E.M. Abad-Villar, M.T. Fernández-Abedul, A. Costa-Garcia, W. Hoffmann, A.E. Guber, D. Herrmann, A. Gerlach, N. Gottschlich, P.C. Hauser, *Analyst* 128 (2003) 1019.